Assessment of regional Arctic ice management with a focus on solar radiation management

L.L. van Dijke[1], H. Hendrikse[1], F. Ypma[2]

[1]Faculty of Civil Engineering and Geosciences, Department of Hydraulic Engineering, Delft University of Technology, Delft 2628 CN, The Netherlands

[2]Arctic Reflections, The Netherlands

Corresponding author: Laura van Dijke, L.L.vanDijke@tudelft.nl

Abstract

The Arctic experiences accelerated warming, resulting in both local and global consequences. This warming leads to a significant reduction in the sea ice cover, contributing to increased absorption of solar radiation and further Arctic warming. Arctic ice management (AIM) offers a geoengineering solution to preserve Arctic sea ice, by flooding existing sea ice during winter, to increase the thickness and extend the ice presence during the summer. This can increase the reflection of incoming solar radiation, making AIM a form of solar radiation management (SRM). Previous theoretical studies focused on AIM simultaneously applied to large parts of the Arctic. However, regional AIM implementation is considered more feasible in terms of logistics and SRM impact. This raises questions about adapting AIM to specific locations, and we have examined the various factors influencing a regional approach. AIM is expected most effective in regions typically becoming ice-free during the summer and the largest impact can be achieved in June. However, under current Arctic conditions, transitional ice regions like the Beaufort Sea, Baffin Bay, and Russian coastal waters remain limited during this time of year. For regional AIM implementation, it is essential to understand the melting rates in different locations, and analysis of the Ice Mass Balance Buoy data reveals an average ice melt rate of 2.4 cm day^{-1} in the Beaufort Sea and 0.85 cm day^{-1} in the Transpolar Drift. To effectively increase ice thickness through AIM, we evaluate the impact of flooding using an AIM growth model, validated through small-scale lab experiments for snow-free conditions. The results indicate that the increase in thickness depends on the initial ice conditions before flooding and the freezing duration afterward. Including snow, the model shows that flooding of snow can enhance the thickening process, which aligns with previous research on snow flooding. Our findings emphasize that for a regional AIM approach, timing and location are key to obtaining a net positive effect and it is expected that just flooding large areas of Arctic Sea ice might not always yield a positive impact.

Keywords: Arctic sea ice, solar radiation management, albedo effect, ice melt, ice thickening

1 Introduction

The Arctic region is warming faster than other latitudes, leading to a rapid decline in Arctic sea ice (Perovich & Richter-Menge, 2009; Screen & Simmonds, 2010; Walsh, 2014). Climate simulations by the Coupled Model Intercomparison Project (CMIP) predict a practically ice-free Arctic ocean in September at least once before 2050 under all scenarios described in the IPCC sixth assessment report (Notz & Community, 2020; IPCC, 2021). However, a more detailed examination of climate models that best match observed Arctic sea ice conditions from recent years indicates that a practically ice-free Arctic ocean might occur as early as 2035 (Docquier & Koenigk, 2021). Additionally, the study by González-Eguino et al. (2017) suggests that Arctic sea ice loss can significantly complicate keeping global warming levels below the 2 °C limit of the Paris Agreement. This phenomenon of increased warming is known as Arctic amplification and has a larger impact than just sea ice loss. It accelerates the melting of land ice and permafrost, directly affecting regional ecosystems. On a global scale, it contributes to increased methane release, rising sea levels, and the occurrence of extreme weather events (Francis & Wu, 2020; Moon et al., 2019). One of the mechanisms contributing to Arctic amplification is the surface albedo feedback, a concept observed as early as 1875, showing that snow and ice reflect more solar radiation than other materials (Croll, 1875). In the Arctic, the variations in albedo can be significant, with average values of 0.06 for the open ocean, 0.5 for bare ice, and 0.9 for ice covered with fresh snow. As sea ice melts, and more open ocean is exposed to solar radiation, the energy absorption increases. While debates persist on whether the albedo feedback is the primary cause of Arctic amplification, (Hall, 2004; Pithan & Mauritsen, 2014; Taylor et al., 2013; Screen & Simmonds, 2010), all studies emphasize the importance of Arctic sea ice.

Geoengineering can help preserve the Arctic ice cover thereby maintaining its albedo. Methods include negative emission technologies (removing carbon dioxide from the atmosphere) and solar radiation management (increasing the amount of reflected solar radiation). One suggestion to preserve the sea ice cover and contribute to solar radiation management is to restore sea ice. This can, for example, be achieved by distributing highly reflective glass microspheres on low reflective sea ice (Field et al., 2018) or by pumping seawater on top of the ice to increase the thickness and extend its presence during the summer (Flannery et al., 1997; Desch et al., 2017), which is known as Arctic ice management (AIM). However, the impact of AIM extends beyond simply increasing the ice thickness, as discussed by Miller et al. (2020). Factors such as the effect on photosynthesis below the ice cover or the introduction of algae in between the original and added ice layer should not be overlooked. Increasing the ice thickness is not a new technology in ice engineering and has been used for many years to construct ice roads and platforms by flooding or spraying the ice with seawater (Masterson, 2009; Nakawo, 1983, 1980). However, it is important to understand that the initial ice thickness for such structures is generally much thicker than what is anticipated for AIM. This variance in starting thickness is expected to impact ice growth during and after the flooding process. Additionally, the coverage required for AIM to have a noticeable impact in terms of SRM is expected to be more extensive.

Continuing the idea of Flannery et al. (1997), Desch et al. (2017) analyzed the feasibility of installing individual wind-powered pumps to flood the ice cover throughout the winter and increase the thickness of 10% of the Arctic ice cover by 1m. Zampieri and Goessling (2019) simulated this with a constant water layer on top of the ice from 21 October to 21 March, resulting in an increase in ice extent, and summer cooling, but also a warming effect during the winter where pumps were active. Alternatively, Pauling and Bitz (2021) used simulations to show that solely flooding the snow layer during September and October significantly reduced the insulating effect of snow during ice growth, resulting in a 70 cm ice thickness increase at the end of the winter. All three studies propose that flooding should start early in winter (September/October) and concern the whole sea ice cover, including multi-year ice (MYI). However, for AIM focused on SRM, a regional approach is expected to be more effective and logistically feasible than aiming for large parts of or the entire Arctic ice cover. Furthermore, the impact on solar radiation reflection may be less pronounced in areas where the ice is naturally thick enough to survive (most of) the summer as compared to transitional ice zones, regions that are ice-covered in winter and transition to open water in summer. While a full consideration of the energy balance due to the thickening of ice through flooding would take several other energy effects, we focus on the Albedo effect and the SRM potential. With the implementation of regional AIM with a focus on SRM in mind, this study examines various factors influencing a regional approach to add insights to the discussion on feasibility and potential impact.

In this study, we take a structured approach to examine the potential of the regional implementation of AIM while focusing on SRM. We begin by identifying regions in the Arctic that are suitable for AIM, considering the ice presence during the summer in combination with the potential for SRM. To gain insights into the AIM needs for extending sea ice presence in the potential regions, the location analysis is followed by an examination of the ice melting rates in different regions using data obtained from the Ice Mass Balance Buoy (IMB) program. Third, to determine the flooding strategy to efficiently obtain an increase in ice thickness, an AIM growth model was derived and validated by small-scale lab experiments. The AIM growth model is expanded to account for the presence of snow, enabling us to compare the impact of AIM in scenarios with and without snow and to compare the results to previous studies. Finally, the above findings are combined to discuss the feasibility of regional AIM with a focus on SRM and related uncertainties as well as the impact of different flooding strategies for varying ice and snow conditions.

2 Potential regions for AIM

The focus of this research is to extend the sea ice presence in transitional ice regions, while aiming for a noticeable SRM effect. When and where the ice presence can be extended depends on the regions with ice in winter and open water in summer, referred to as transitional regions. Figure 1 identifies these transitional regions for June, July, and August, by comparing the ice edge for the first day of these months to March 1^{st} of the corresponding year and overlaying the obtained transitional regions between 2013 and 2022. The images are generated using the sea ice edge product of the Ocean and Sea Ice Satellite Application Facility (OSI-SAF) and considering a concentration threshold value of 70%.

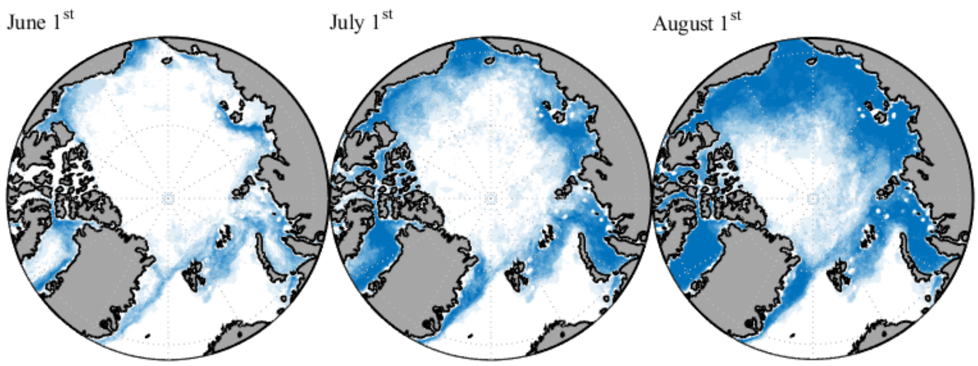

Figure 1. Indication of transitional ice regions over 2013-2022 for June 1^{st}, July 1^{st} and August 1^{st} compared to the 1^{st} of March ice area of the corresponding year. The image is generated using data defining the sea ice edge of the Ocean and Sea Ice Satellite Application Facility OSI SAF.

The East coast of Greenland shows a potential area of interest considering ice presence, however, there is generally an ocean current exporting ice southwards, where ice is expected to melt quickly. Excluding this area, most other regions find themselves in either the Northern Sea Route (Russian waters) or the Northwest Passage (along west Greenland, Canada, and Alaska). Prolonging the ice in these regions can be disadvantageous for marine transport or Arctic exploitation, making the region selection also an economic and political matter. These regions come with the challenges of possibly operating in thick ice during winter or in the vicinity of icebergs. At the same time, these regions occur relatively close to land which offers advantages from a logistics viewpoint. The transitional regions shown do not account for sea ice dynamics, and applying AIM might be necessary at different locations than where the actual effect is seen.

To quantify the potential for SRM, we consider the increase in solar radiation reflection as a direct effect. A full energy balance would also include latent and sensible heat effects during both the winter and summer, which can be visualized using climate simulations as shown in earlier studies by Zampieri and Goessling (2019); Pauling and Bitz (2021). For example, AIM is known to have a warming effect when the ice is flooded with sea water during the winter, however, to define if there could be a net benefit from regional AIM we first need to understand the possible impact of AIM during the summer on a regional scale. How much solar radiation can be reflected depends on the location, dimension, moment, and duration of the extended ice presence. The reflection is estimated using the solar radiation received at the location of interest, the insolation 'I'. This requires the solar constant $S = 1366$ W m^{-2}, latitude 'ϕ', declination angle $\delta = -23.45 \cdot cos(\frac{360}{365.25}(day + 10))$ and hour angle $HA = 15 \cdot (t_{hr} - 12)$, where '$t_{hr}$' is the solar time in hours given on a 24-hour clock. Some of the incoming radiation will be reflected by the clouds before it reaches the surface, which is estimated based on the cloud fraction $f_{cl} = 0.81$ and cloud albedo 'a_{cl}', which is considered comparable to the ice-albedo (He et al., 2019). Constant values for the cloud fraction and albedo are considered, however, these are expected to vary with time and location. Combining the expression results in the following formula:

$$I = [S \cdot cos(\phi)cos(\delta)cos(HA) + sin(\phi)sin(\delta)] \cdot (1 - f_{cl}a_{cl}) \ \ [\mathrm{W\ m^{-2}}], \tag{1}$$

where a negative insolation is considered as $I = 0$ W m^{-2}. The energy absorbed in the Arctic depends on the albedo 'a' of ice, land, and open ocean (average values of 0.6, 0.5, and 0.06 are assumed) and their corresponding areas 'A'. To determine the potential of increasing the energy reflection by extending the ice presence, the difference in albedo between sea ice and open ocean is of interest. Average values of 0.6 and 0.06 for the ice and open ocean are considered, however, the sea ice albedo is expected to vary during the summer from approximately 0.85 for ice covered with cold snow to 0.2 after which the ice is expected to rapidly melt away (Perovich & Polashenski, 2012). The difference in energy reflected per unit area can be estimated by considering the duration for which the ice presence is extended.

$$\Delta E_{\text{refl}} = (a_i - a_o) \cdot I \cdot \Delta t \;\; [\text{J m}^{-2},] \tag{2}$$

where 'I' depends on the day of year and 'Δt' equals the duration that the ice presence is extended during the summer. Figure 2 illustrates how the potential increase in solar radiation reflection depends on when the ice presence is extended and the duration of ice extension. The contour lines approach a vertical profile when increasing the duration of ice extension, this indicates that increasing the thickness beyond a specific value during winter time will not result in a net positive contribution of AIM when the total energy balance is considered.

Based on Figure 2, the largest effect in terms of solar radiation reflection can be obtained in regions that normally become ice-free in June, while extending the ice presence in August has a significantly reduced effect. At the same time, Figure 1 indicates the transitional ice regions at the beginning of June are limited in extent. This is another factor impacting the feasibility of the application of AIM for the specific purpose of SRM. On the other hand, it is expected that due to continuing global warming, these regions may expand in size in the coming years.

3 Regional Summer Ice Melting Rates

With locations for regional AIM defined it is necessary to understand the melting of ice in those regions in order to define how much ice growth is to be generated to extend the presence of sea ice with a specific desired duration. Both Desch et al. (2017) and Maykut and Untersteiner (1971) provided a relation for ice decay based on air tem-

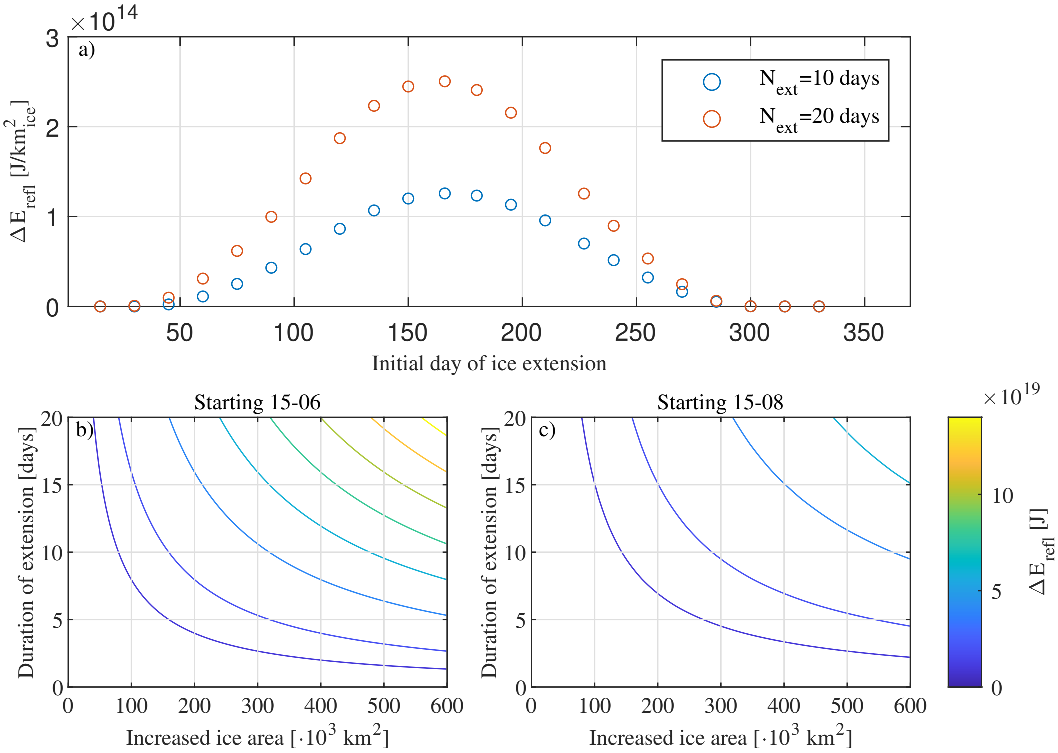

Figure 2. Estimate of the change in energy reflection due to AIM at 75°N, depending on the initial day the ice presence is extended (a), and when the increased area and duration of ice extension are varied when the ice presence is extended starting from June 15 (b) or August 15 (c).

perature and solar radiation (long-wave and short-wave radiation). Using these relations to predict future ice decay requires daily weather forecasts concerning air temperature, cloud coverage, and snow conditions. This complicates accurate predictions of the expected ice decay for specific regions. Even though long-wave radiation is generally larger in magnitude than shortwave radiation, both Desch et al. (2017) and Maykut and Untersteiner (1971) indicated that the ice decay is controlled by solar radiation (shortwave radiation) because the net contribution of the incoming and outgoing long-wave radiation (radiative temperature of the air and ice) is generally small. The solar radiation at a specific location on Earth depends on the latitude and time of year, and a relation between these elements and ice decay might be present. Here we investigate the possibility of defining average melting rates for specific locations which can aid in the judgement of the feasibility of regional AIM. This research considers an empirical approach using buoy measurements from the IMB program (Perovich et al., 2022) to identify average ice melting rates for different regions. For the analysis, the ice is assumed to start melting at the surface once the snow layer has disappeared. This assumption proves relatively accurate when studying the data, except for Buoys 2012G, 2012J, 2013A, 2013F, and 2015E. For these buoys, a snow cover remains throughout the melting season, and the moment of initial melt was determined by examining the data and identifying the start manually. The measurements for most buoys stop before the end of the melting season, though this is not expected to affect the average location-specific melting rate significantly. For the data that run beyond the melt season, the final measurements within two centimeters of the minimal ice thickness are excluded from the analysis. This limit is considered to account for minor variations in the measurements and is only applied to data exceeding the melting season. The obtained drift tracks during the melting phase for all buoys considered in this study are shown in Figure 3. Buoys 2012E, 2012M, 2013A, 2013C, and 2015A are excluded from the analysis because they cannot be grouped or are considered too close to land relative to other buoys in the specified region, which can impact ice melt. Furthermore, Buoy 2013B and 2006D are eliminated because of significant unexpected increases or decreases in ice thickness measurements. Even though the positions of the buoys do not entirely match the regions of interest defined earlier, the buoys are divided into two groups: The Beaufort Sea and the Transpolar Drift as indicated in Figure 3.

The ice decay is evaluated as a function of the day of the year, and for each buoy, a linear trend line based on the least-squares method is fitted through the ice thickness data. Figure 4 shows the average measured ice thickness per day, before the melting starts and during the melting phase. The symbols indicate the start and end of the ice melting, in between which the ice melting rates are calculated. Starting with the Beaufort Sea, a clear trend is visible, and only the measurements from three buoys deviate from this: 2012G, 2012H, and 2013F. As mentioned earlier, a snow layer between 0.05 m and 0.1 m remains throughout the melting phase for Buoys 2012G and 2013F, which can explain the smaller gradient. For 2012H, the beginning of ice decay is defined for a snow layer reaching 0 m. However, the second half of the melting phase shows the formation of a new snow layer. When analyzing only the ice decay stage free of snow, the melting rate slightly increases to 1.6 cm day^{-1}, which still deviates from the general trend for a currently unknown reason. Based on the general trend, a melting rate between 2.1 and 2.7 cm day^{-1} is considered a good approximation for average ice decay in the Beaufort Sea during the melting season after the snow has disappeared.

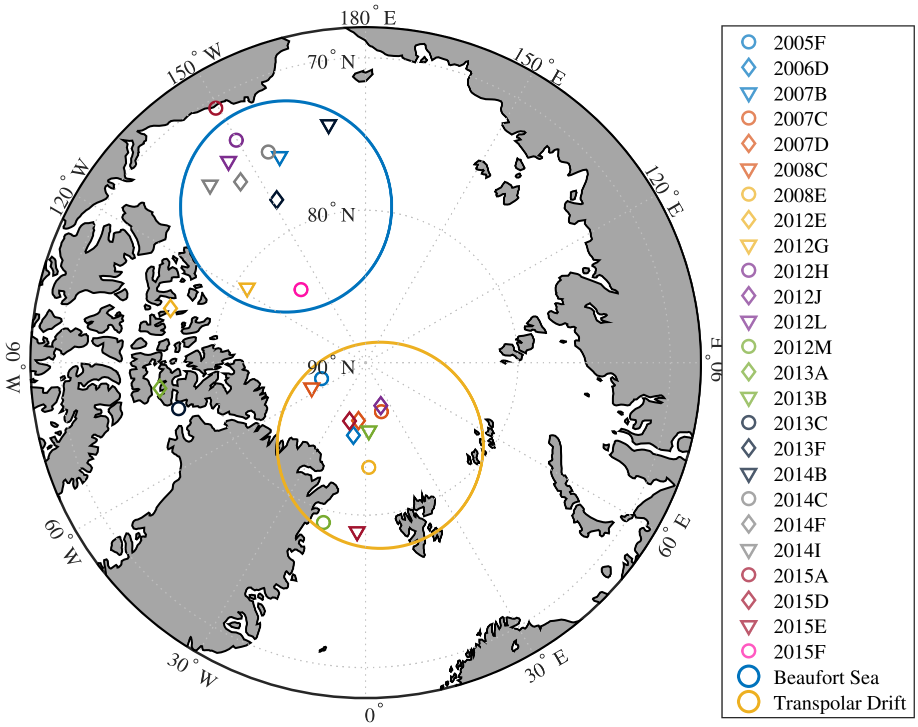

Figure 3. Location of the final measurement taken during the melting season for the buoys analyzed. Which represents the end of the data set or when the ice thickness was no longer decreasing.

Similarly, a trend is visible for ice in the Transpolar Drift. Three buoys follow a slightly steeper trend: 2008E, 2015D, and 2015E. Buoy 2015E is relatively far south and receives more solar radiation compared to the other buoys in this region, which can explain the increase in ice decay. For buoys 2008E and 2015D, the data examined do not show a clear explanation for the steeper trend. Furthermore, the snow conditions in the Transpolar Drift vary throughout the summer. As mentioned earlier, buoys 2015E and 2012J have a continuous snow layer throughout the measurements. For buoys 2005F, 2008C, and 2008E, the snow layer disappears, but snow falls during the melting phase. The three remaining buoys, 2007C, 2007D, and 2015D experience ice decay under snow-free conditions. These varying conditions do not show proportionate effects on the ice decay, and a general trend is visible among most buoys. Eliminating the largest deviating trends, results in an expected average ice melting rate between 0.7 and 1.0 cm day^{-1} after the snow has disappeared.

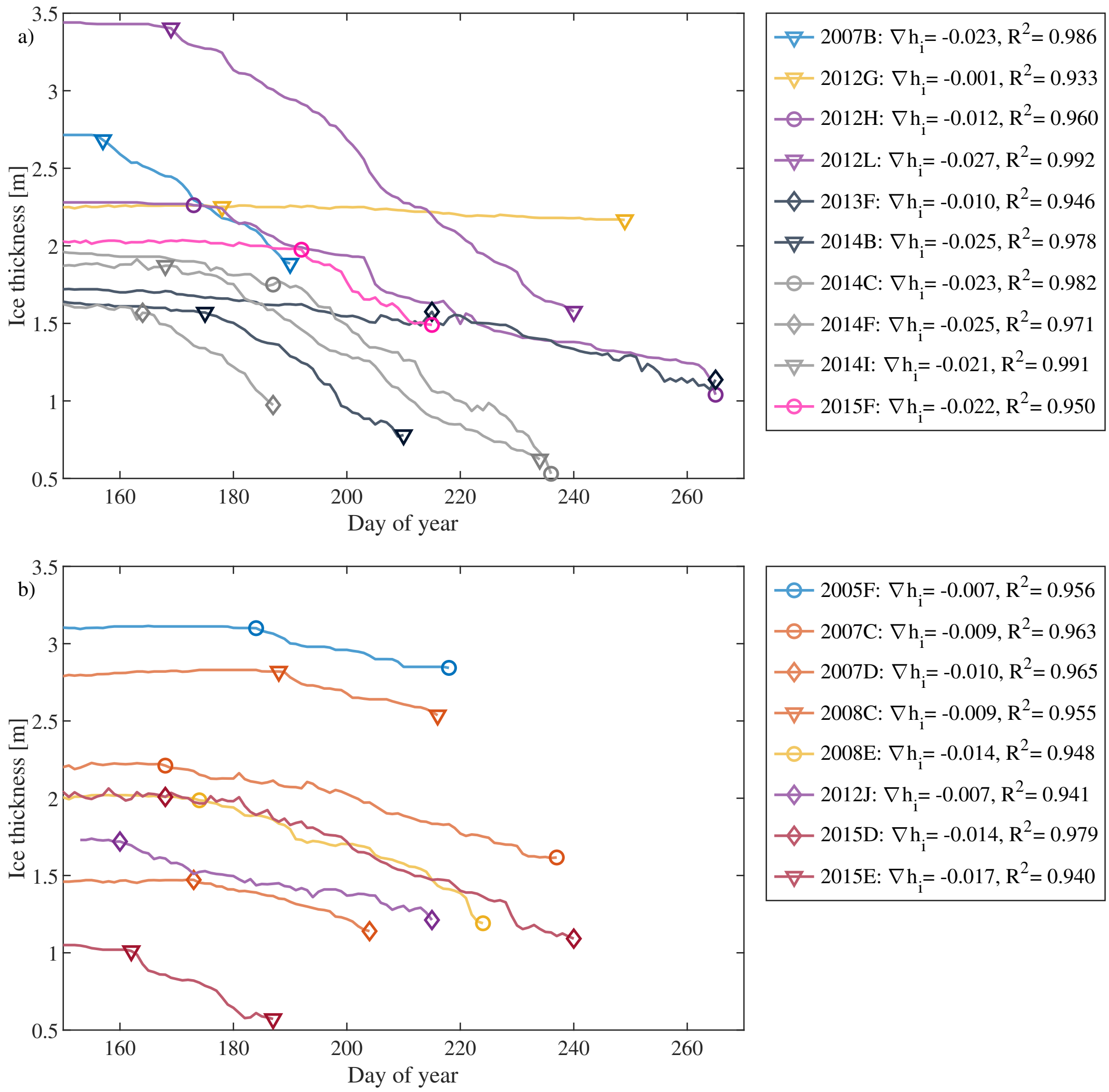

Figure 4. Comparison between melting rates for the Beaufort Sea (a) and the Transpolar Drift (b). The symbols indicate the first and last measurement during the melting season, in between which the melting rate is calculated.

When comparing both regions, it can be seen that ice in the Beaufort Sea experiences faster ice decay (average 2.4 cm day^{-1}) than ice in the Transpolar Drift (average 0.85 cm day^{-1}), which is expected due to differences in latitude, oceanic heat flux, and snow conditions. First, the buoys analyzed in the Transpolar Drift are between 85 and 90 °N, while the buoys in the Beaufort Sea are further South (approximately 75°N). Ice located southward receives more solar radiation during the summer accelerating ice decay. Secondly, Lin and Zhao (2019) determined an average oceanic heat flux of 16.8 W m^{-2} in the Beaufort Sea and 7.7 W m^{-2} in the Transpolar Drift, indicating that the bottom melt in the Beaufort Sea exceeds the bottom melt in the Transpolar Drift. Finally, the varying but generally increased snow conditions in the Transpolar Drift can act as a protective cover and reduce the melting rate. The trends for both locations are considered reliable for ice thicknesses of 0.5 m and above. They might suit thinner ice, but this can not (yet) be confirmed as data on ice thicknesses below 0.5 m were not available in the used dataset. It is noteworthy that there is no clear acceleration or deceleration of ice melt when comparing the different years. This indicates that solar radiation might indeed control ice melt and the values derived are considered applicable at present.

With the derived regional melting rates, the necessary ice thickness increase by AIM can be determined depending on the desired duration of ice extension. The difference in melting rate between the two locations emphasizes that the locations can benefit from different AIM strategies. For example, extending the ice presence in the Transpolar Drift with 10 days would require an ice thickness increase of 8.5 cm (10 days $\cdot$ 0.85 cm day^{-1}). However, the transitional ice area in the Transpolar Drift is currently limited as shown in Figure 1, yet it is expected to increase during the coming years. The Beaufort Sea offers a larger transitional ice area but requires an ice thickness increase of 24 cm for the same duration of ice extension (10 days). The regions defined in Section 2 that become ice-free in June and July are generally located further South and also closer to land than the position of the buoys analyzed. This can influence the melting rates at the specific locations illustrated in Figure 1, potentially resulting in an accelerated ice melt, which indicates that more AIM is required.

4 Increasing the Ice Thickness

The concept of AIM is to increase the ice thickness during winter by flooding existing ice. Both Desch et al. (2017) and Zampieri and Goessling (2019) considered constant flooding of the ice cover throughout the winter. Alternatively, Pauling and Bitz (2021) analyzed flooding during specified months but limited the flooding height to the snow depth. This paper analyzes the flooding of existing ice, in the absence of snow and for different snow scenarios, to define how AIM can be used most efficiently. The snowfall during September and October typically forms a significant snow depth on top of the ice cover that survived the preceding summer. As shown by Pauling and Bitz (2021), the ice cover can be significantly increased by flooding this snow layer early during the season. However, the onset of seasonal ice growth typically occurs in October or November, which is after we observe the substantial increase in snow depth in the IMB data.

The constant snow depth observed in the data does not exclude snowfall as the snow layer might also condense and there might be snowfall after the initial formation of the seasonal ice, however, we cannot exclude the possibility of encountering bare sea ice. Therefore, we also analyze the flooding of bare sea ice, as this might not yield the same positive effects. Furthermore, a regional approach is seen as a more realistic representation of actual operations, where installations aim for specific areas instead of general flooding of the Arctic ice cover and it is anticipated that different regions could benefit from different flooding strategies.

4.1 Theory of Ice Growth

The theory describing ice growth was already derived in 1891 by Stefan (1891) and is still widely used for analyzing ice growth. In this concept, ice formation is initiated when the temperature falls below the freezing point of water. For seawater, generally used values vary between -1.6 to -1.8 °C depending on the water salinity. An initial ice layer is formed, and the ice continues to grow downwards. Due to the cold air temperatures in winter, the ice surface cools down, while the bottom of the ice cover remains at the freezing temperature. This results in a temperature profile in the ice cover, which is assumed linear. When ice grows at the bottom of the ice cover, latent heat is released into the ice and conducted upwards towards the colder surface (Fourier's law), where the heat is transferred to the atmosphere. For Stefan's law, the latent heat released and heat conducted upwards are balanced, resulting in the following relation:

$$-\rho_i l_i \frac{dh_i}{dt} = \frac{k_i}{h_i}(T_a - T_f) + q_{\text{ocean}}, \tag{3}$$

where $rho_i = 917$ km m^{-3} is the density of ice, $l_i = 3.34 \cdot 10^5$ J kg^{-1} the latent heat and $k_i = 1.9$ W m^{-1} K^{-1} thermal conductivity (Ono, 1967). Furthermore, h_i represents the ice thickness, T_f is the freezing temperature (which is also the temperature at the bottom of the ice cover), and T_a refers to the atmospheric temperature. Finally, there is an oceanic heat flux at the ice bottom, but this flux is neglected during ice growth. In reality, the ice surface temperature does not equal the atmospheric temperature. To account for this, a heat transfer coefficient 'C_t' can be included. Various values for the heat transfer coefficient have been used: 24 W m^{-2} K^{-1} (Maykut, 1986), 30 W m^{-2} K^{-1} (Desch et al., 2017) and an experimentally derived coefficient of 15.2 W

m^{-2} K^{-1} (Lozowski et al., 1991). These variations mainly impact thin ice growth and for longer freezing durations the ice thicknesses are similar. Furthermore, the ice thickness is expressed in terms of freezing degree days (FDD), which is the cumulative sum of the number of degrees below freezing during each day, $FDD = \int_0^t (T_f - T_a)$, and can be converted to seconds using the factor $\alpha = 86400$. Finally, the expression can be adapted to account for snowfall during the winter. Snow forms an insulating layer on top of the ice cover and slows down the ice growth. This results in the expression (Maykut, 1986):

$$H^2 + \left(\frac{2k_i}{k_s}h_s + \frac{2k_i}{C_t}\right)H = \frac{2k_i}{\rho_i l_i}\alpha FDD, \tag{4}$$

where k_s is the thermal conductivity of snow, and h_s is the snow layer thickness. This derivation describes how ice grows when insulated, which will be used for deriving an AIM ice grow model.

For the development of ice roads and platforms, the focus is on the additional sensible and latent heat release and the temperature inside the added ice layers to optimize the ice growth rate at the surface (due to flooding), while generating sufficient bearing capacity (Szilder & Lozowski, 1989a; Nakawo, 1983, 1980). Likewise, Desch et al. (2017) stated that the additional latent heat release affects the ice growth at the surface; however, they expect the impact to be slight. Additionally, they emphasized that the added water layer creates a blanketing effect slowing down the natural ice growth. Because of these two reasons, Desch et al. (2017) concluded that the increased ice thickness due to constant flooding is 70% of the flooding height. The blanketing effect is generally not mentioned in the ice growth derivations for ice structures, which can be due to differences in ice thickness. Previous studies considering the formation of ice structures often refer to initial ice thicknesses of 3m and the effect of flooding on the temperature profile in the original ice cover is expected to remain in the top 0.5m (Nakawo, 1980; Szilder & Lozowski, 1989b, 1989a). Both the initial and increased ice thickness for AIM are expected thinner and the impact on the natural ice growth during and after flooding can be significant.

Small-scale experiments for the flooding of thin ice have been conducted and Lozowski et al. (1991, p. 31) stated,"*if the ice onto which the layer is flooded is cold, the freezing process will proceed both from above due to convective heat transfer at the surface, and* *from below due to conduction of heat into the underlying ice*". During the experiments, they investigated changes in the temperature profile of the ice during the flooding process. When the ice cover is flooded with relatively warm water, the temperature profile approaches a vertical profile and restores towards a linear profile afterward. Based on their findings, it is expected that depending on the initial ice thickness, the flooding height, and the temperature difference between the ice and floodwater, the temperature profile does or does not fully reach a vertical profile after flooding.

4.2 Analytical AIM Growth Model

The obtained ice thickness due to AIM depends on both the flooded ice growth, the ice growth at the ice-ocean interface, and the ice growth afterward. As Lozowski et al. (1991) did not describe ice growth at the ice-ocean interface during or after flooding the ice, their derivation is not adopted, but the theory is used to develop a new AIM growth model. To allow for small-scale experiments, snow is not accounted for in this first derivation. Considering heat is conducted from warmer to colder surroundings results in the following three ice growth processes (see also Figure 5):

1. Ice growth at the ice-ocean interface 'd1'. Heat is conducted upwards into the original ice resulting in ice growth downwards. Depending on the minimum temperature along the temperature profile in the ice cover.
2. Ice growth at the AIM-ice interface 'd2'. Heat is conducted downwards into the original ice, resulting in ice growth upwards. Depending on the minimum temperature along the temperature profile in the ice cover.
3. Ice growth at the air-AIM interface 'd3'. Similar to the initial formation of an ice layer. There is convective heat transfer to the atmosphere, followed by heat conduction upwards after a thin ice layer has formed at the top of the flooded layer, resulting in ice growth downwards.

To create the AIM growth model, the effect of flooding on the temperature profile in the ice requires further understanding. Assuming only vertical heat transfer, a 1D problem analysis could determine the temperature profile. However, flooding causes a sudden change in the boundary conditions at the AIM-ice interface, which increases the complexity. For this reason, an upper and lower limit for the ice growth is derived, as illustrated in Figure 5. Compared to the theoretical processes, the ice growth at the AIM-ice interface 'd2' is excluded for the upper and lower limit scenarios to simplify the derivation. In the case of the upper limit scenario, the flooded layer is modeled similarly to thin ice growth. The ice growth at the bottom of the original layer is modeled as if the ice is insulated by a time-dependent mixture of ice and floodwater (similar to ice growth insulated with a snow layer, but using the properties of the flooded layer instead). This is expected to overestimate the ice thickness because the change in temperature profile is expected to slow down or temporarily interrupt the ice growth 'd1'. For the lower limit scenario, a vertical temperature profile is assumed during the flooding phase, which interrupts ice growth 'd1'. This scenario is expected to underestimate the ice growth 'd1' because ice growth at the ice-ocean interface continues to some extent depending on the changed temperature profile. The height of the total water layer added is referred to as the flooding height. The floodwater is expected to expand when it freezes resulting in a slightly thicker layer, which is referred to as the AIM thickness.

4.3 Small Scale Lab Experiments

To validate the upper and lower limit scenarios introduced in the previous section, experiments were conducted in a cold room at Delft University of Technology. Three identical coolers were used with inside dimensions of 458 x 396 x 325 mm (LxWxH). Each cooler was filled with 45 L of tap water, leaving enough margin for flooding the ice. The tap water was mixed with Aquaforest Sea Salt to obtain a salinity of 30.5 ($\pm$ 0.5) ppt. The salinity was measured using the Greisinger GMH 3431, which accounts for the water temperature. The coolers were placed in the cold room which maintained an average temperature of -20°C and experienced a defrost cycle of $\pm$ 1.5 °C. A time-lapse camera recording was used to identify initial ice formation, which can be observed by the formation of a thin film at the water's surface. The ice thickness was measured using a ruler and a margin of $\pm$1 mm is included in the results. Furthermore, a Greisinger G1710 Thermometer was used to obtain the ice surface temperature and water temperature underneath the ice. The accuracy of the surface temperatures measured is questioned as ice formed on the thermometer during measurements, and therefore the surface temperatures were not used for the analysis. For future experiments, a thermistor array as used in the experiment by Lozowski et al. (1991) would be recommended instead.

Figure 6 shows the experimental setup and an example of water temperature measurements. Some remarks on the ice growth are that the ice was left to grow to the sides

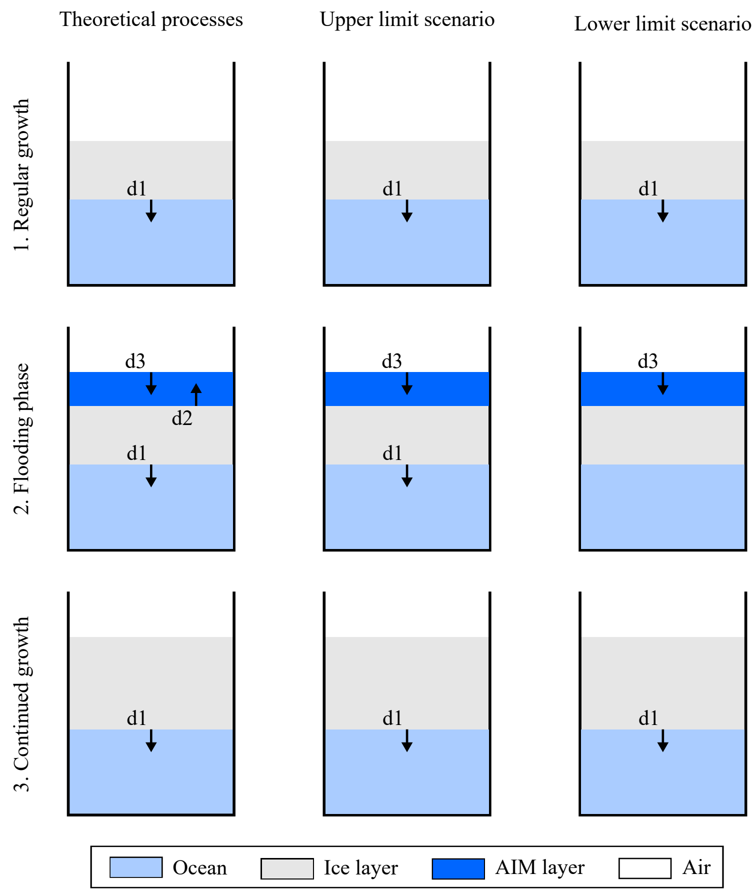

Figure 5. Theoretical ice growth processes during AIM and during the upper and lower limit scenario. Step 1 shows regular ice growth according to Stefan's law. Step 2 shows the flooding phase with various ice growth processes simultaneously, and Step 3 indicates continued ice growth according to Stefan's law.

of the cooler, which was necessary for flooding the ice. Furthermore, the coolers provided insulation at the sides and bottom to avoid cooling and ice formation. Finally, the grain structure was not accounted for, because the effect on the ice growth process was expected to be minor. In practice, the ice would be flooded with water retrieved from underneath the ice. This setup does not allow for this and therefore an additional cooler was prepared with saline water, which was cooled down to near freezing temperature of -1.65°C.

A reference experiment was conducted to confirm the natural ice growth in the cold room with Stefan's law. Two coolers were placed in the cold room and the ice thickness was measured for three consecutive mornings. The experimentally derived transfer coefficient of 15.2 W m^{-2} by Lozowski et al. (1991) matched our measurements and was used for further analysis. During the reference experiment, it was noticed that the ice

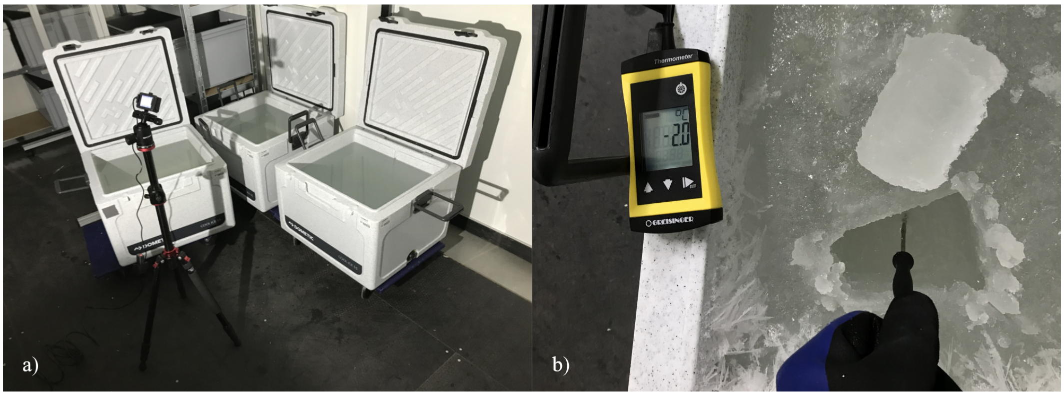

Figure 6. a) Experimental setup including the camera to record initial ice formation. b) Example of an ice sample and water temperature measurements.

surface remained slightly wet throughout the experiment, which might be the result of water being pushed through the ice due to pressure build-up underneath as ice grows downwards in a confined space. This is not experienced when growing fresh water (tap water) ice in the same cold room, so the saline ice might be more porous, and/or brine channels allow the water to flow through the ice. Furthermore, the salinity of the water underneath the ice increases significantly due to salt rejection when the ice grows, which is the consequence of working with a finite volume and does not occur, to this extent, in the Arctic. To account for this, the decreasing freezing temperature due to an increase in salinity is included in the FDD calculations.

To validate the derived ice growth model in the previous section, four different experiments were conducted. The ice was either flooded instantly or flooded incrementally and flooding occurred after 24hr or 48hr of cooling. Keeping the cooling time constant resulted in slightly different initial ice thicknesses, because the water temperature inside the coolers, when placed in the cold room, showed some variations. Figure 7 shows ice samples after multiple days of draining and clearly shows the AIM layer on top of the original ice layer after instant flooding and the various sub-layers after incremental flooding. The ice samples were obtained from different experiments and cannot be compared in terms of total ice thickness.

For both flooding scenarios, the added layer seems to be whiter, which can result from a salinity difference between the original and AIM layer or more air entrapped in the AIM layer. Field measurements related to the salinity of flooded sea ice have shown that after flooding the salinity of the flooded ice reduces to approximately 20ppt (Gani et al., 2019; Nakawo & Frederking, 1981). Nakawo (1980) observed that the salinity remained constant during the winter until the temperatures of the ice started to increase and the salinity had dropped to 5 ppt by late June. It is unsure if the whiteness of the AIM will maintain over time, if it does the AIM layer can be beneficial for the albedo effect. At the same time, if there is a significant increase when the melting starts, the ice melt might actually be accelerated.

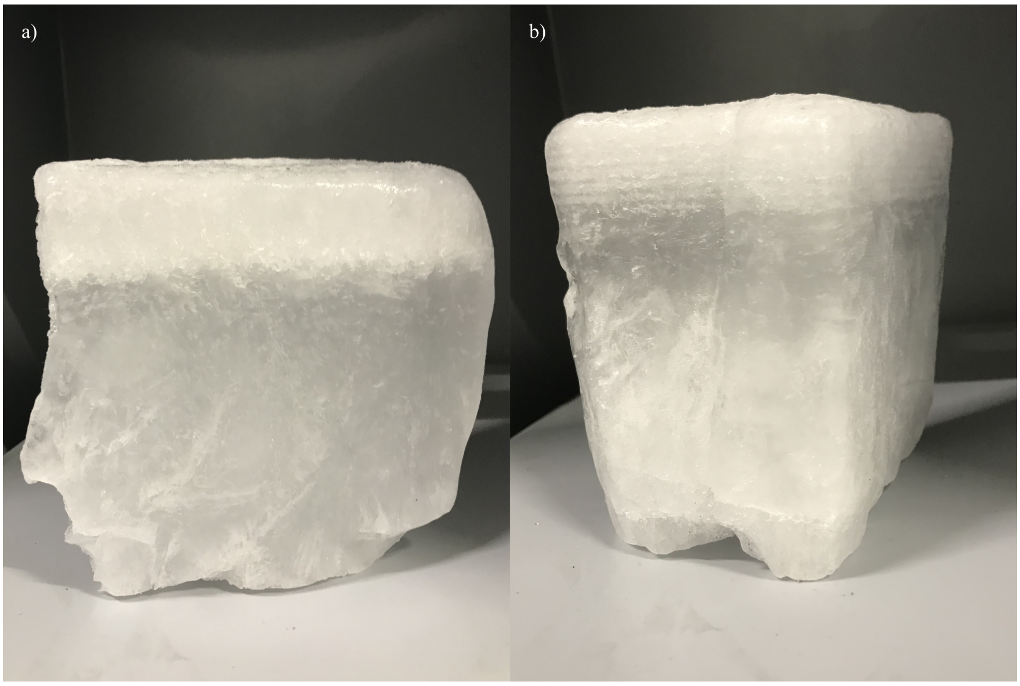

Figure 7. Ice samples during different experiments after multiple days of draining. a) Ice after instant flooding. b) Ice after incremental flooding showing multiple thin layers.

A reference cooler was used during each AIM experiment to monitor natural ice growth and each test was replicated, however, the initial ice thickness for each duplicate is not exactly equal due to a difference in water temperature prior to cooling. If the reference cooler showed deviating measurements, there is a possibility that external factors have influenced the experiment and the results were considered invalid. Figure 8 shows the results for each valid experiment, and the replicated results can be found in Appendix A. Some deviations for both the reference and test coolers were observed during the second to last measurements during Test III and IV (which were conducted simultaneously). As the last measurement for the reference cooler does confirm normal ice growth and the duplicate experiment does not indicate similar deviations, the second to last observation is considered a measurement error. Figure 8 shows an ice thickness between the upper and lower boundary at the end of the flooding phase for all experiments. However, when ice growth continued the ice thickness approached the lower boundary estimation and followed Stefan's law afterward. To ensure this delay was not the result of applied forces when cutting the ice, a fifth test was conducted for two coolers simultaneously and is shown in Appendix A. The ice thickness of each cooler including AIM is measured only once to eliminate the impact of the sawing process. The results are in line with the previous measurements and ensure the cutting process has no significant impact on the ice growth. Instead, the delay observed can be caused by additional time required before the two ice layers have fully merged causing a temporary boundary. Alternatively, additional time might be required before the temperature profile is restored, which was also observed by Lozowski et al. (1991) and this could temporarily slow down the ice growth.

4.4 Scaling of AIM growth model and the impact of snow

The AIM growth model follows the phases as illustrated. When the desired initial ice thickness is reached, flood water is applied in sub-layers of 2 cm, which is comparable to layer thicknesses used during the construction of ice roads and platforms (Masterson, 2009; Nakawo, 1983). The ice growth in a sub-layer depends on the number of FDD passed. To balance the accuracy of the ice growth and the computational time, an interval of 0.4 FDD is considered. A different interval might be required if the sub-layer thickness is changed. When the sub-layer is completely frozen, the original and added ice layer are considered as a single ice cover and the next sub-layer is simulated. This process is repeated until the desired AIM thickness is reached. After the last sub-layer is frozen, the ice cover follows Stefan's law.

Using the 2 m height air temperature of the ECMWF European Reanalysis V5 (ERA5) (Hersbach et al., 2020) and a freezing temperature of -1.65°C recent years indicate 2500 to 3000 FDD during a winter season between 60° to 90°N. Figure 9 shows the AIM growth model for various initial ice thicknesses simulated for 2750 FDD, considering a heat transfer coefficient of 24 W m^{-2} K^{-1} (Maykut, 1986). The AIM growth model shows the effective ice thickness increase grows for thicker initial ice, due to the non-linear growth rate of ice. Thin ice grows faster than thicker ice, therefore, flooding thinner ice disrupts the naturally fast growth resulting in a reduced effective ice thickness increase. For the same reason, the difference between the upper and lower limit scenario decreases for thicker

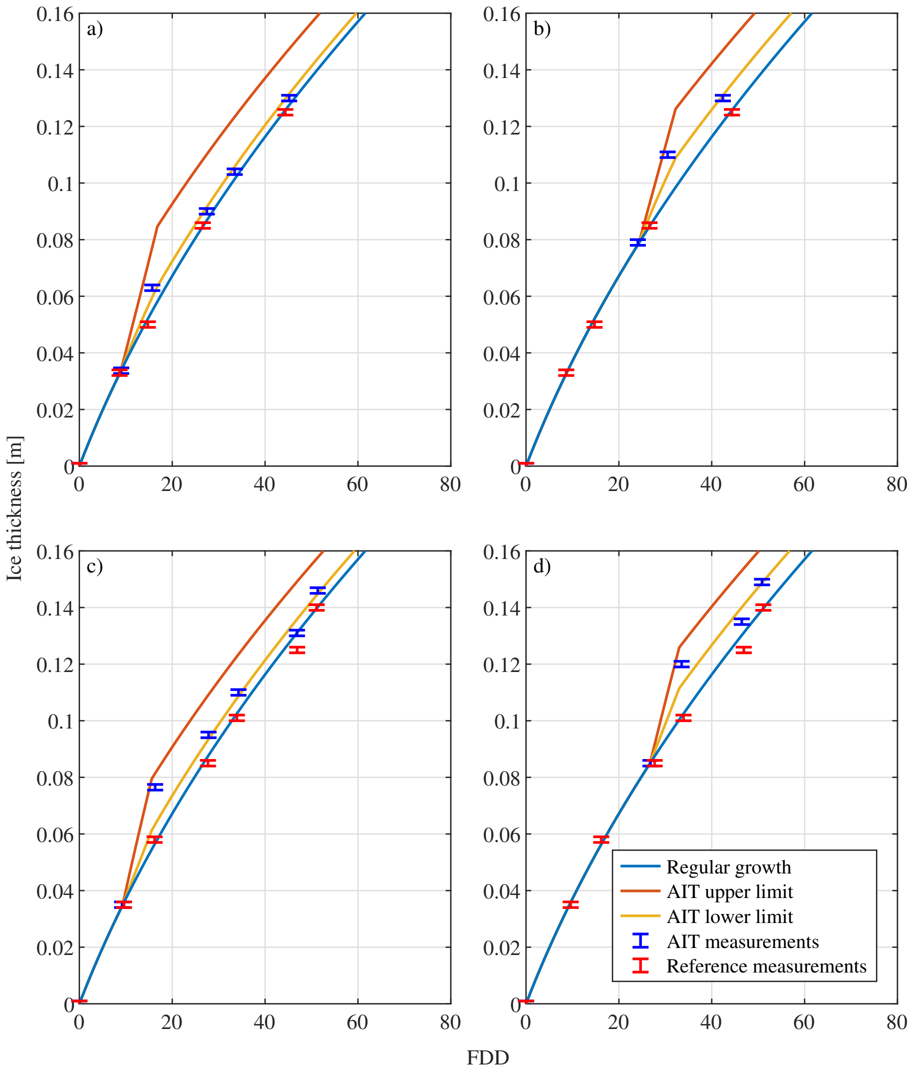

Figure 8. Results of the different AIM experiments. a) Test I - Instant flooding after 24h cooling. b) Test II - Instant flooding after 48h cooling. c) Test III - Incremental flooding after 24h cooling. d) Test IV - Incremental flooding after 48h cooling.

initial ice and the effective ice thickness increase reduces over time after the flooding phase. This indicates that the effective ice thickness increase depends on the initial ice thickness prior to flooding and the freezing duration after the flooding phase. The effect of various flooding heights is compared using the thickness increase expressed as a fraction of the flooding height, as shown in Table 1. Both the maximum increase (directly after the flooding phase) and the effective increase 1000 FDD after flooding are shown. For each initial ice thickness, the maximum fractional increase is similar for various flooding heights (with slightly larger variations for $H_i = 0.2$ m) and increases with initial ice thickness. 1000 FDD after flooding started, the fractional increase is larger for the flooding of thicker initial ice conditions and also increases with flooding height.

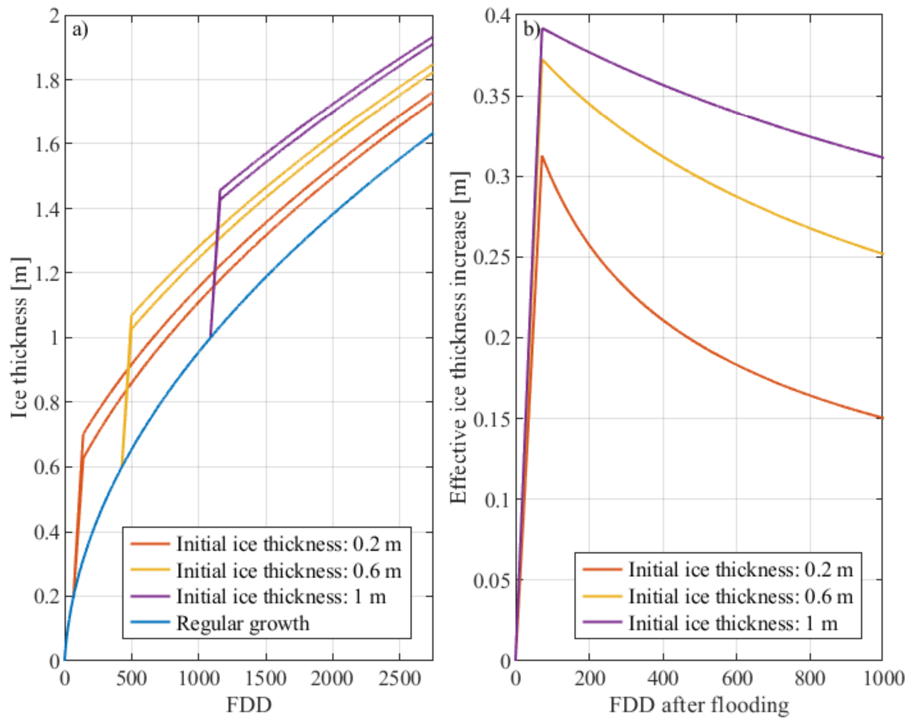

Figure 9. Ice growth with 0.4 m flooding height applied on different initial ice thicknesses showing both the lower and upper limit scenarios (a) and the development of effective ice thickness increase over FDD after flooding started, for the lower limit scenario (b).

Using the Community Earth System Model (CESM), (Pauling & Bitz, 2021) showed that flooding the snow layer during the fall or early winter can actually amplify the thickening process. A snow layer can be included in our growth model, but some assumptions are required concerning the created slush and snow-ice layers. Following Leppäranta (1993), it is assumed that the slush thickness equals the flooding height, there is no compression in the snow, slush properties are taken as the weighted average of the ice-snow combination and the properties for snow-ice are considered equal to regular sea-ice properties. For the flooding phase, this means that the original ice layer can be covered with a combination of slush, snow, added ice, and water in a ratio depending on the initial conditions before flooding and the flooding height. To include snow in the AIM model a snow density of 330 kg m^{-3} and snow conductivity of 0.31 W m^{-1}K^{-1} are considered.

Table 1. Fractional increase of the flooding height 'H_{fw}' directly after the flooding phase *(and 1000 FDD after flooding started)* for different initial ice thicknesses 'H_i' considering the lower limit scenario under snow-free conditions.

	$H_i = 0.2$ m		$H_i = 0.6$ m		$H_i = 1.0$ m	
H_{fw}=0.40 m	0.70	*0.34*	0.84	*0.57*	0.88	*0.70*
H_{fw}=0.70 m	0.73	*0.44*	0.84	*0.62*	0.88	*0.73*
H_{fw}=1.00 m	0.74	*0.51*	0.84	*0.67*	0.88	*0.76*

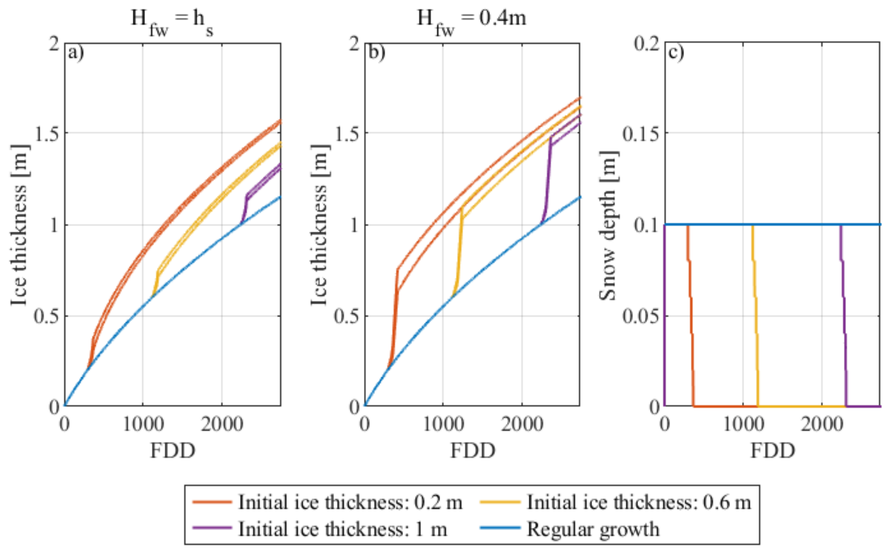

Figure 10. Impact of different flooding strategies considering a constant snow cover

Comparing the conditions with and without snow implies that depending on the conditions, different flooding strategies will result in the thickest ice. In the absence of snow, the effective ice thickness increase will be larger for thicker initial ice conditions occurring later during the winter for seasonal ice. Furthermore, our model indicates that in the absence of snow, the effective ice thickness increase reduces over time after the flooding is completed, as shown in Figure 9. This is different for a situation with a constant snow layer and only the snow layer is flooded, as shown in Figure 10. For the situation illustrated, flooding the snow layer enhances the ice-thickening effect, which is similar to the findings by (Pauling & Bitz, 2021). Additionally, the effective increase is larger when the snow layer is flooded on thin initial ice, which occurs early during the winter. When we keep on flooding the ice after the snow layer is fully flooded ($H_{fw} > h_s$), the growth model indicates early flooding will have a slight benefit compared to flooding later in the season, but the final ice thicknesses are relatively similar (Figure 10.b).

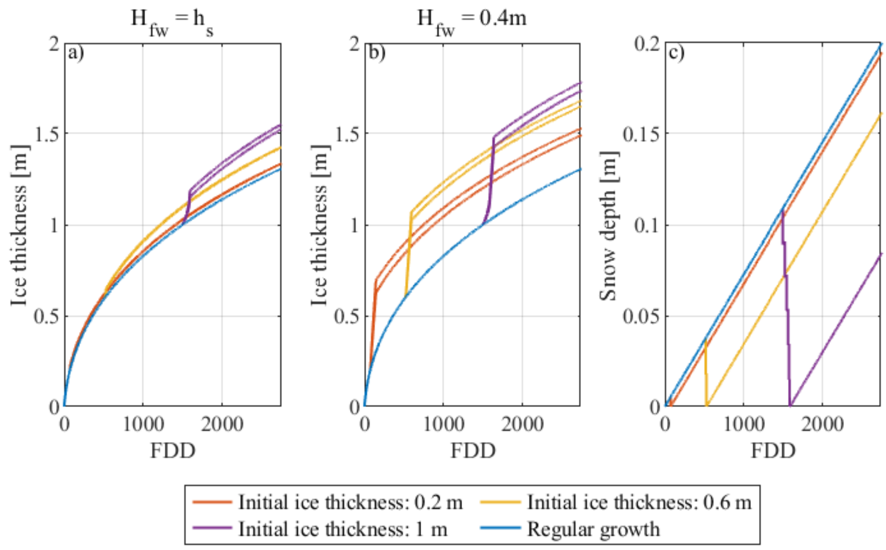

Figure 11. Impact of different flooding strategies considering an increasing snow layer

It is worth noting that flooding solely the snow layer (0.1m) early in the winter or flooding the ice with 0.4m does not result in a significant difference in the final ice thickness. Finally, Figure 11 illustrates that for a linearly increasing snow depth, it is more efficient to initiate flooding later during the winter. Noteworthy, for the situation as illustrated in Figure 11.b, the effective ice thickness increase reduces over time for initial ice thicknesses of 0.2m and 0.6m, however, increases for the initial ice thickness of 1.0m.

5 Discussion on the feasibility of AIM for SRM purposes

Arctic ice management (AIM) with a focus on Solar Radiation Management (SRM) is expected more effective and feasible in terms of logistics when adopting a regional approach, as opposed to aiming for the entire ice cover. Consequently, the question is raised whether every location will equally benefit from the same AIM approach. In this study, we have examined the various aspects that can shape a regional AIM approach and we discuss the key findings necessary when proceeding with the regional application of AIM.

The most substantial impact in terms of SRM is expected in the transitional ice zones, characterized as regions that are ice-covered in winter and transition to open water during the summer. For the reason that the difference in albedo between sea ice and open water is significant. Due to the solar position, the possible increase in solar radiation reflection due to the extension of sea ice presence is largest in June and decreases towards the end of summer. Analysis of these transitional regions at various time points throughout the summer shows that the transitional ice regions in early June are still limited under current Arctic conditions. However, it is anticipated that these regions will expand during the coming years due to the changing climate.

AIM is expected to cause a warming effect during the winter, which should be outweighed by the impact in terms of SRM during the summer to yield an overall positive effect. However, the impact of AIM in terms of solar radiation reflection during the summer is not linear over time. This indicates that extending the ice presence for twice as long does not necessarily result in double the impact in terms of solar radiation reflection. Consequently, extending the duration of ice presence beyond a specific threshold does not yield a net-positive contribution to SRM, when considering the overall energy balance.

To obtain the desired increase in solar radiation reflection during the summer, AIM should increase the ice thickness to a certain threshold depending on the anticipated ice melt rate. IMB Buoy data provides insights indicating that in select regions, the ice melt rate can be quantified in centimeters per day and, it is expected that the latitude, oceanic heat flux, and snow conditions have a dominating role in this context. It is noteworthy that the locations covered by the data set do not exactly align with the transitional ice regions considered for the regional implementation of AIM. Typically the regions of interest find themselves further South which can imply a higher melting rate compared to the data analyzed. Nevertheless, it can be anticipated that the criteria for extending the ice presence are within the order of magnitude of a few centimeters per day. No melt data was obtained for flooded sea ice and the application of AIM might influence the melt rate. During AIM implementation the ice cover is flooded with seawater, which results in a high salinity in the added ice layer, which might accelerate the ice melt during the summer. Based on the findings presented by (Nakawo & Frederking, 1981), it is likely that the salinity remains around 20ppt when the ice temperatures remain low. However, based on the same observations, significant desalination of the added ice is expected to occur towards the beginning of summer, and it remains uncertain if the salinity will significantly impact the melt rate.

Research by (Pauling & Bitz, 2021) demonstrated that flooding the snow layer early during the winter (September-October) can enhance the ice-thickening effect, which can be a valuable use of AIM. Analyzing the snow depth measurements obtained from the previously selected IMB buoys shows a seasonal pattern, which was also observed by Warren et al. (1999) for measurements obtained from Soviet drifting stations. The pattern indicates a rapid increase in snow depth from late August to October, which remains fairly constant until April and May when a moderate increase can be observed again. This results in the formation of a notable snow layer early during the winter atop the ice that survived the preceding summer melt, which can be flooded as (Pauling & Bitz, 2021) suggest. However, the onset of seasonal ice growth is not expected until October or November and is not necessarily covered by this significant snow depth. There might be snowfall after the initial formation of the seasonal ice, however, we cannot exclude the possibility of bare sea ice. Therefore, we also analyze the flooding of bare sea ice, as this might not yield the same positive effects. The formulated AIM growth model emphasizes the pivotal role of snow conditions atop the ice cover before and after the application of AIM in determining the most advantageous flooding strategy. We have examined three scenarios to illustrate how defined conditions can benefit from varying flooding strategies. The first scenario shows that in the absence of snow flooding the sea ice early during the winter significantly disrupts the natural ice growth process, resulting in a reduced increase in ice thickness compared to thicker initial ice conditions occurring later during the winter. Additionally, the effective increase decreases over time after flooding is completed. Consequently, in the absence of a snow cover, it becomes more efficient to apply AIM later in the winter season. In contrast, the second scenario assumes a constant snow depth before flooding occurs and we find that flooding of a constant snow layer amplifies the thickening effect due to AIM, which is similar to the observations by Pauling and Bitz (2021). This indicates that flooding early during the winter is the most effective approach. Furthermore, exceeding the initial snow depth during early winter flooding does not necessarily yield a substantial difference in the final ice thickness. This aspect has a crucial role in the overall energy balance for AIM, as more flooding will likely increase the warming effect in the winter, which is ineffective if it does not yield a substantial increase in thickness compared to solely flooding the snow layer. Lastly, we can consider a linearly increasing snow layer throughout the winter. For this scenario, it is anticipated that postponing flooding to later in the winter will yield the most substantial increase in ice thickness, and flooding beyond the snow depth can result in a notable difference. Whether there is an amplifying or reduction in effective ice thickness increase over time, depends on the snow depth, initial ice conditions, and flooding height. Irrespective of the scenario, it is essential to bear in mind that the formation of a protective snow cover late in the winter season is vital to obtain a positive impact in terms of SRM. If, due to AIM, there is no snow cover at the beginning of the melting season, the ice is expected to start melting earlier in the season diminishing the ice cover throughout the summer, instead of extending the sea ice presence.

Considering the factors discussed regarding the regional implementation of AIM, it becomes clear that a location-specific strategy has the potential to yield a substantial increase in ice thickness, consequently extending the presence of sea ice during the summer. Contradictory, a simplistic approach of uniform flooding (parts of) the ice cover may prove disadvantageous for the overall energy balance by AIM, particularly in terms of the warming effect during winter and the summer solar radiation reflection. In the continuation of a regional AIM approach, simulations using climate models are vital for understanding the various effects AIM can induce throughout the year and assessing whether the overall impact of AIM is favorable or not. In addition to the impact related to solar radiation management or the warming effect of flooding the ice cover, it is important to recognize that the implementation of AIM can induce other challenges when it comes to monitoring the ice cover or utilizing data that is reliant on passive microwave sensors. These difficulties arise as the flooded layer on top of the ice cover can make it difficult to distinguish the sea ice from open water.

6 Conclusion

6.1 Summary

The decreasing ice cover in the Arctic shows the effects of climate change. However, it also contributes to the rapid temperature increase in this region, as the decreasing ice cover allows more solar radiation to be absorbed. Using geoengineering to preserve the sea ice cover during the summer can increase the reflection of solar radiation, which can therefore be referred to as a solar radiation management (SRM) technique. One suggestion is to use Arctic ice management (AIM), which aims to flood the ice cover thereby increasing the thickness of existing ice during the winter and extending the duration of ice presence during the summer. This study considered the various factors influencing a regional approach of AIM, by focusing on transitional ice regions, regions with ice during winter and open water during the summer. Analyzing the transitional regions between 2013 and 2022 showed that currently the Beaufort Sea, the Baffin Bay the Russian waters are potential areas where AIM with a focus on SRM can yield the largest impact. To gain a better understanding of AIM requirements in potential regions, the location analysis was followed by an examination of the melting rates for different locations. Our analysis, based on data from the Ice Mass Balance Buoy (IMB) program, indicates that the rate of summer ice melt varies by location due to differences in latitude, oceanic heat flux, and snow conditions. For the Beaufort Sea and Transpolar Drift region, we defined average melting rates of 2.4 and 0.85 cm day^{-1} for ice thicknesses of 0.5m and above. These melting rates provide insights into the necessary increase in ice thickness required at the end of winter.

In order to determine the most effective use of AIM on a regional scale, we developed an AIM growth model to compare the impact of different flooding strategies in relation to the initial ice and snow conditions. Small-scale lab experiments were conducted to validate our growth model in the absence of snow. The least favorable scenario in terms of water requirements is that of bare sea ice, which may occur when newly formed ice, which holds the most potential for SRM, has not yet experienced any snowfall. For this scenario, our model suggests that it is more effective to flood the ice cover later in the winter compared to early winter flooding. Furthermore, the effective ice thickness increase is largest directly after flooding but decreases over time for the remainder of the winter. This is in contrast to a scenario with a constant snow depth prior to flooding. In this case, flooding the snow layer amplifies the ice-thickening process, and the most substantial increase in ice thickness at the end of the winter is achieved when flooding takes place early in the winter. Finally, if we assume a linear increase in snow depth, our model indicates that it is again more effective to use AIM later in the winter. Irrespective of the scenario, it is essential to bear in mind the importance of a snow layer developing during at the end of winter. If, due to AIM, there is no snow cover at the beginning of the melting season, the ice is expected to start melting earlier in the season diminishing the ice cover throughout the summer, instead of extending the sea ice presence.

Our study shows that adapting AIM to regional conditions can result in an efficient flooding strategy and thereby potentially reduce the known winter warming and aid the energy balance due to AIM throughout the year. For the summer effect, an analysis of the potential energy reflection shows that the necessary effort to maintain the ice until the end of summer might outweigh the additional benefit in terms of increased energy reflection as the solar radiation reaching the Arctic is significantly reduced towards the end of the summer. For these reasons, the potential for a net positive effect of regional AIM targeting SRM remains, but the analysis does highlight potential pitfalls that could lead to a negative impact of such an operation. Additionally, we should be aware that the net effect due to AIM might change as a result of the changing Arctic conditions in the coming years.

6.2 Recommendations

Based on the findings of this research, several aspects for further research have appeared. For instance, including regional AIM in climate models can provide valuable insights into the full energy balance influenced by AIM. Besides the impact AIM can have in terms of solar radiation reflection and the expected cooling effect, the extended ice cover could possibly reduce ocean warming, influencing neighboring ice regions, and promoting initial ice growth. However, AIM is also known to have a warming effect during the winter and potentially impact cloud behavior and precipitation, aspects for which we have not yet fully anticipated the impacts on the ice cover and the energy balance. Furthermore, considering the dynamics of ice could provide guidance on where AIM should be applied to maximize the benefits in terms of SRM. For these reasons, we recommended conducting climate simulations to comprehensively assess the impact of the regional use of AIM and aid in the potential and feasibility discussion.

Thus far, we have exclusively validated the AIM growth model on a small scale and in the absence of snow. Therefore, it is recommended to conduct experiments on a larger scale under varying snow and no-snow conditions, to validate the full model. Additionally, we advise conducting a comprehensive analysis of the ice properties of the increased ice, including aspects such as ice strength, ice salinity, ice albedo, how these properties evolve over time, and the possible impact on ice melt or growth on a large scale.

An essential technical question that remains open is the distribution of the water on top of the ice cover. The water has to be distributed on top of the ice cover over a significant area. However, both the ice surface and atmospheric temperatures are below the floodwater temperature, which can complicate the distribution of a thin layer of seawater and the ice area is typically not a smooth and flat surface, including the possibility of individual ice floes. Technologies used in the construction of ice roads and platforms (spraying or flooding) can provide solutions for the distribution during AIM, however, the coverage considered for AIM is significantly larger. Desch et al. (2017) considered the installation of individual pumps distributed across the Arctic in its entirety to reach the desired coverage. We expect that a regional AIM approach is more feasible in terms of logistics and individual pumps or pumps in combination with vessels might be a solution.

Finally, the large scale of AIM can lead to (unwanted) side effects if not thoroughly analyzed. For example, Miller et al. (2020) mentioned a reduction of photosynthesis underneath the ice cover by blocking more sunlight and introducing algae in between the original and added ice layer, which should not be overlooked. Additionally, regionally extending the ice presence can affect (new) shipping routes and daily life in nearby villages. Deliberately defining the duration of ice extent depending on the location can keep these disadvantages limited and potentially increase opportunities related to the increased ice presence.

Appendix A Results of duplicate experiments

The results from the duplicate experiments and the additional experiment to exclude sawing effects are shown in Figure A1. Each duplicate encountered equal cooling time prior to flooding, due to variations in water temperatures this resulted in similar but slightly different initial ice thicknesses.

Data availability statement

The OSI SAF sea ice edge data was obtained from the OSI SAF FTP server:
`ftp://osisaf.met.no/archive/` (OSI SAF)
Ice thickness data of the CRREL-Dartmouth Mass Balance Buoy Program was obtained from: `http://imb-crrel-dartmouth.org/archived-data/` (Perovich et al., 2022)
The ECMWF European Reanalysis V5 data set was obtained from:
`https://ClimateReanalyzer.org` (Hersbach et al., 2020).

Acknowledgments

We would like to thank Cody Owen for his significant contribution to the design of the test setup and his valuable assistance during the experiments.

Disclosure of interests

After the completion of this study, one of the coauthors, Fonger Ypma, founded an impact-driven company named Arctic Reflections, a startup that builds upon the research findings presented in this paper and other relevant studies. The establishment of Arctic Reflections took place independently of the research process and has no influence on the study, analysis, or interpretation of the results. Hayo Hendrikse and Laura van Dijke solely have a voluntary advisory role towards Arctic Reflections, offering insights based on their knowledge and experience. The authors would like to emphasize that all research findings are open access, ensuring full transparency and accessibility.

References

Croll, J. (1875, 6). Climate and time in their geological relations; a theory of secular changes of the earth's climate. *Nature*, *12*, 141-144. doi: https://doi.org/10.1038/012141a0

Desch, S. J., Smith, N., Groppi, C., Vargas, P., Jackson, R., Kalyaan, A., ... Hartnett, H. E. (2017, 1). Arctic ice management. *Earth's Future*, *5*, 107-127. doi: https://doi.org/10.1002/2016EF000410

Docquier, D., & Koenigk, T. (2021, 12). Observation-based selection of climate models projects arctic ice-free summers around 2035. *Communications Earth and Environment*, *2*. doi: https://doi.org/10.1038/s43247-021-00214-7

Field, L., Ivanova, D., Bhattacharyya, S., Mlaker, V., Sholtz, A., Decca, R., ... Katuri, K. (2018, 6). Increasing arctic sea ice albedo using localized reversible geoengineering. *Earth's Future*, *6*, 882-901. doi: https://doi.org/10.1029/2018EF000820

Flannery, B. P., Kheshgi, H., Marland, G., & Maccraken, M. C. (1997). Geoengineering climate. In R. G. Watts (Ed.), *Engineering response to global climate change* (p. 379-427).

Francis, J. A., & Wu, B. (2020, 11). Why has no new record-minimum arctic sea-ice extent occurred since september 2012? *Environmental Research Letters*, *15*, 114034. doi: https://doi.org/10.1088/1748-9326/abc047

Gani, S., Sirven, J., Sennéchael, N., & Provost, C. (2019, 12). Revisiting winter arctic ice mass balance observations with a 1-d model: Sensitivity studies, snow density estimation, flooding, and snow ice formation. *Journal of Geophysical Research: Oceans*, *124*, 9295-9316. doi: 10.1029/2019JC015431

González-Eguino, M., Neumann, M. B., Arto, I., Capellán-Perez, I., & Faria, S. H. (2017, 1). Mitigation implications of an ice-free summer in the arctic ocean. *Earth's Future*, *5*, 59-66. doi: https://doi.org/10.1002/2016EF000429

Hall, A. (2004, 4). The role of surface albedo feedback in climate. *Journal of Climate*, *17*, 1550-1568. doi: https://doi.org/10.1175/1520-0442(2004)017<1550:TROSAF>2.0.CO;2

He, M., Hu, Y., Chen, N., Wang, D., Huang, J., & Stamnes, K. (2019, 7). High cloud coverage over melted areas dominates the impact of clouds on the albedo feedback in the arctic. *Scientific Reports*, *9*, 9529. doi: https://doi.org/10.1038/s41598-019-44155-w

Hersbach, H., Bell, B., Berrisford, P., Hirahara, S., Horányi, A., Muñoz-Sabater, J., … Thépaut, J. (2020, 7). The era5 global reanalysis. *Quarterly Journal of the Royal Meteorological Society*, *146*, 1999-2049. doi: 10.1002/qj.3803

IPCC. (2021). Summary for policymakers [Book Section]. In V. Masson-Delmotte et al. (Eds.), *Climate change 2021 – the physical science basis. contribution of workin group i to the sixth assessment report of the intergovernmental panel on climate change* (p. 3-32). Cambridge University Press. doi: 10.1017/9781009157896.001

Leppäranta, M. (1993, 3). A review of analytical models of sea-ice growth. *Atmosphere-Ocean*, *31*, 123-138. doi: 10.1080/07055900.1993.9649465

Lin, L., & Zhao, J. (2019, 6). Estimation of oceanic heat flux under sea ice in the arctic ocean. *Journal of Ocean University of China*, *18*, 605-614. doi: https://doi.org/10.1007/S11802-019-3877-7

Lozowski, E., Jones, S., & Hill, B. (1991, 11). Laboratory measurements of growth in thin ice and flooded ice. *Cold Regions Science and Technology*, *20*, 25-37. doi: 10.1016/0165-232X(91)90054-K

Masterson, D. M. (2009, 9). State of the art of ice bearing capacity and ice construction. *Cold Regions Science and Technology*, *58*, 99-112. doi: https://doi.org/

10.1016/j.coldregions.2009.04.002

Maykut, G. A. (1986). The surface heat and mass balance. In *The geophysics of sea ice* (p. 395-463). Springer US. doi: https://doi.org/10.1007/978-1-4899-5352-0_6

Maykut, G. A., & Untersteiner, N. (1971). Some results from a time-dependent thermodynamic model of sea ice. *Journal of Geophysical Research*, *76*(6), 1550–1575. doi: https://doi.org/10.1029/JC076i006p01550

Miller, L., Fripiat, F., Moreau, S., Nomura, D., Stefels, J., Steiner, N., … Vancoppenolle, M. (2020, 9). Implications of sea ice management for arctic biogeochemistry. *Eos*, *101*. doi: https://doi.org/10.1029/2020EO149927

Moon, T. A., Overeem, I., Druckenmiller, M., Holland, M., Huntington, H., Kling, G., … Wong, G. (2019, 3). The expanding footprint of rapid arctic change. *Earth's Future*, *7*, 212-218. doi: https://doi.org/10.1029/2018EF001088

Nakawo, M. (1980, 8). Heat exchange at surface of built-up ice platform during construction. *Cold Regions Science and Technology*, *3*, 323-333. Retrieved from `https://linkinghub.elsevier.com/retrieve/pii/0165232X80900385` doi: 10.1016/0165-232X(80)90038-5

Nakawo, M. (1983). Criteria for constructing ice platforms in relation to meteorological variables. *Cold Regions Science and Technology*, *6*(3), 231-240. doi: https://doi.org/10.1016/0165-232X(83)90044-7

Nakawo, M., & Frederking, R. (1981). The salinity of artificial built-up ice w e by successive floodings of sea water. In *Iahr international symposium on ice, ii* (p. 516-525).

Notz, D., & Community, S. (2020, 5). Arctic sea ice in cmip6. *Geophysical Research Letters*, *47*. doi: https://doi.org/10.1029/2019GL086749

Ono, N. (1967). Specific heat and heat of fusion of sea ice. *Physics of Snow and Ice: proceedings*, *1*(1), 599-610.

OSI SAF. (2023). *Global sea ice edge, osi-402-d* [dataset]. EUMETSAT Ocean and Sea Ice Satellite Application Facility. (Accessed in 2023) doi: doi:10.15770/EUM_SAF_OSI_NRT_2005

Pauling, A. G., & Bitz, C. M. (2021, 10). Arctic sea ice response to flooding of the snow layer in future warming scenarios. *Earth's Future*, *9*. doi: https://doi.org/10.1029/2021EF002136

Perovich, D. K., & Polashenski, C. (2012, 4). Albedo evolution of seasonal arctic sea ice. *Geophysical Research Letters*, *39*. doi: 10.1029/2012GL051432

Perovich, D. K., Richter-Menge, J., & Polashenski, C. (2022). *Observing and understanding climate change: Monitoring the mass balance, motion, and thickness of arctic sea ice* [dataset]. Retrieved from `http://imb-crrel-dartmouth.org` (Accessed in 2022)

Perovich, D. K., & Richter-Menge, J. A. (2009, 1). Loss of sea ice in the arctic. *Annual Review of Marine Science*, *1*, 417-441. doi: https://doi.org/10.1146/annurev.marine.010908.163805

Pithan, F., & Mauritsen, T. (2014). Arctic amplification dominated by temperature feedbacks in contemporary climate models. *Nature Geoscience*, *7*, 181-184. doi: https://doi.org/10.1038/NGEO2071

Screen, J. A., & Simmonds, I. (2010, 4). The central role of diminishing sea ice in recent arctic temperature amplification. *Nature*, *464*, 1334-1337. doi: https://doi.org/10.1038/nature09051

Stefan, J. (1891). Ueber die theorie der eisbildung, insbesondere über die eisbildung im polarmeere. *Annalen der Physik*, *278*, 269-286. doi: https://doi.org/10.1002/andp.18912780206

Szilder, K., & Lozowski, E. (1989a, 1). Optimizing the growth thermodynamics of artificial floating ice platforms. *Ocean Engineering*, *16*, 99-115. doi: https://doi.org/10.1016/0029-8018(89)90045-0

Szilder, K., & Lozowski, E. P. (1989b). A time-dependent thermodynamic model of the build-up of sea-ice platforms. *Journal of Glaciology*, *35*, 169-178. doi: https://doi.org/10.3189/s0022143000004457

Taylor, P. C., Cai, M., Hu, A., Meehl, J., Washington, W., & Zhang, G. J. (2013, 9). A decomposition of feedback contributions to polar warming amplification. *Journal of Climate*, *26*, 7023-7043. doi: https://doi.org/10.1175/JCLI-D-12-00696.1

Walsh, J. E. (2014). Intensified warming of the arctic: Causes and impacts on middle latitudes. *Global and Planetary Change*, *117*, 52-63. doi: https://doi.org/10.1016/J.GLOPLACHA.2014.03.003

Warren, S. G., Rigor, I. G., Untersteiner, N., Radionov, V. F., Bryazgin, N. N., Aleksandrov, Y. I., & Colony, R. (1999). Snow depth on arctic sea ice. *Journal of Climate*, *12*, 1814-1829. doi: https://doi.org/10.1175/1520-0442(1999)012<1814:SDOASI>2.0.CO;2

Zampieri, L., & Goessling, H. F. (2019, 12). Sea ice targeted geoengineering can delay arctic sea ice decline but not global warming. *Earth's Future*, *7*, 1296-1306. doi: https://doi.org/10.1029/2019EF001230

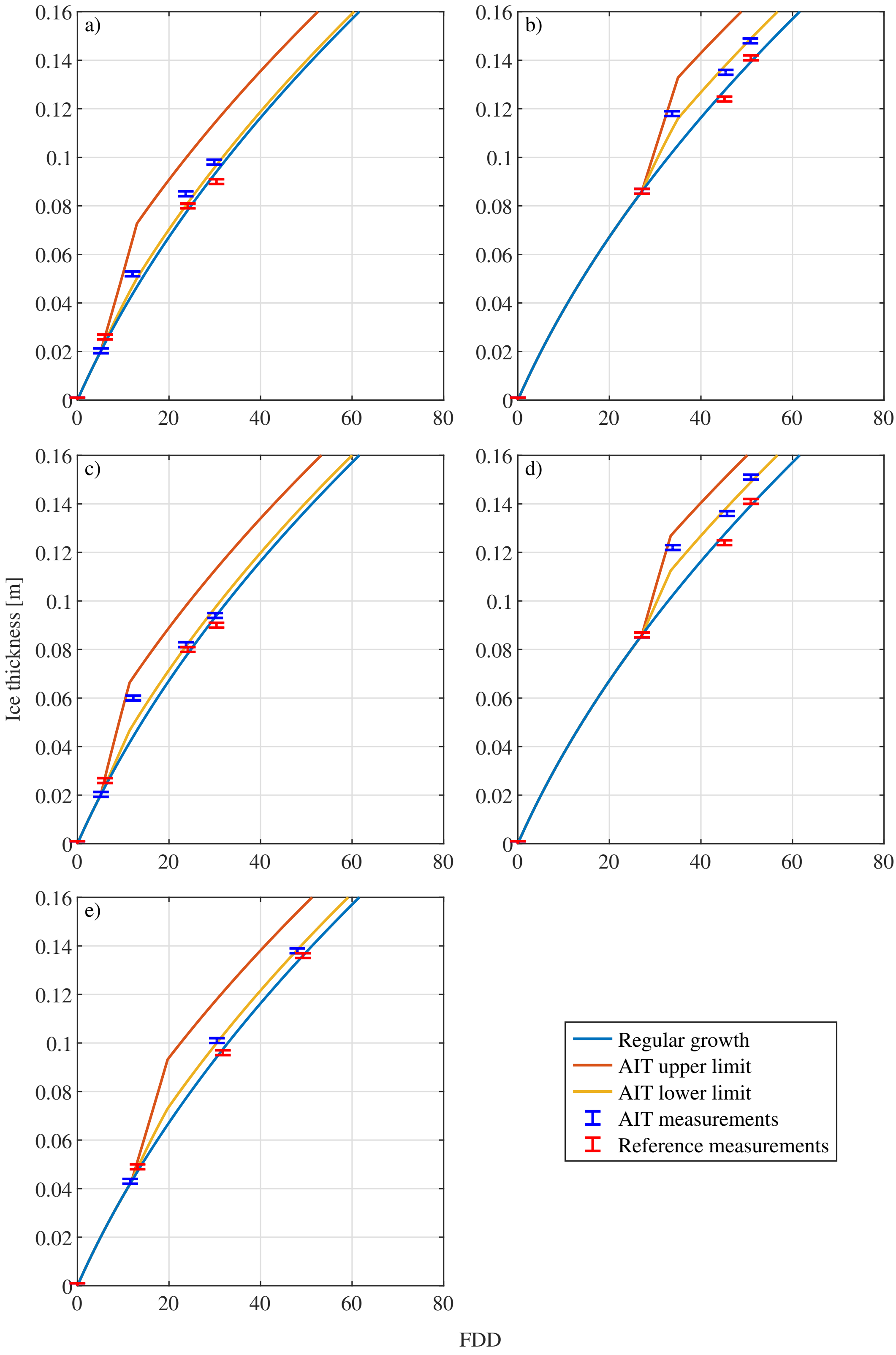

Figure A1. Results of the duplicate AIM experiments. a) Test IB - Instant flooding after 24h cooling. b) Test IIB - Instant flooding after 48h cooling. c) Test IIIB - Incremental flooding after 24h cooling. d) Test IVB - Incremental flooding after 48h cooling. e) Test V: Instant flooding of two coolers to exclude a significant impact of sawing effects.